Lattice mismatch and crystal growth of monoclinic $KY_{1-x}Yb_x(WO_4)_2/KY(WO_4)_2$ layers by liquid phase epitaxy

2008 J. Phys.: Condens. Matter 20 225004

(http://iopscience.iop.org/0953-8984/20/22/225004)

J. Phys.: Condens. Matter **20** (2008) 225004 (10pp) doi:10.1088/0953-8984/20/22/225004

Lattice mismatch and crystal growth of monoclinic $KY_{1-x}Yb_x(WO_4)_2/KY(WO_4)_2$ layers by liquid phase epitaxy

O Silvestre, A Aznar, R Solé, M C Pujol, F Díaz and M Aguiló

Física i Cristal·lografia de Materials (FiCMA), Universitat Rovira i Virgili (URV), Campus Sescelades c/Marcel·lí Domingo, s/n, E-43007-Tarragona, Spain

E-mail: magdalena.aguilo@urv.cat

Received 14 November 2007, in final form 27 February 2008
Published 16 April 2008
Online at stacks.iop.org/JPhysCM/20/225004

Abstract

Monoclinic layers of $KY_{1-x}Yb_x(WO_4)_2$ with a thickness of up to 330 μm were grown on $KY(WO_4)_2$ substrates by liquid phase epitaxy (LPE) using $K_2W_2O_7$ solvent. The layers grown from solutions of up to 7.5 at.% substitution of Y by Yb generally had flat surfaces on {010} and {110} crystal faces with no macroscopic defects at the layer/substrate interface. Already at 10 at.% of Yb substituting Y, some defects at the interface tend to appear and increase for higher concentrations. The layers grown on {310} and $\{\bar{1}11\}$ faces show more growth instabilities even at low Yb concentrations. The thermal evolutions of the lattice mismatches between the epilayer and the substrate for {010}, {110}, {310} and $\{\bar{1}11\}$ faces were calculated to range from 0.55% at 1273 K to −0.31% at 298 K. The optical spectroscopic studies carried out with these samples agree well with Yb-doped KYW bulk crystals, the measured absorption and calculated (by the reciprocity method) emission cross-sections at 981 nm with $E \parallel N_m$ being $\sigma_{abs} = 12.5 \times 10^{-20}$ cm^2 and $\sigma_{em} = 15.8 \times 10^{-20}$ cm^2, respectively.

(Some figures in this article are in colour only in the electronic version)

1. Introduction

Lasers based on thin films have the advantage of high beam quality with high efficiency, making them suitable to obtain high power with low thermal lensing [1].

Interest in laser crystals containing Yb^{3+} as an active ion has been increasing in the last few years. This is due to the small quantum defect and the absence of excited state absorption and upconversion processes as a consequence of its simple electronic level structure. Yb^{3+} has a unique excited level, $^2F_{5/2}$, with an energy difference of about 10 000 cm^{-1} from the $^2F_{7/2}$ ground level. In addition, its large absorption band at around 980 nm permits pumping with high power InGaAs laser diodes [2, 3].

The crystals of the family of monoclinic double tungstates, such as $KGd(WO_4)_2$, $KY(WO_4)_2$ (hereafter KYW) and $KLu(WO_4)_2$, are excellent hosts for Yb^{3+} ions [4–6]. It is also possible to obtain thin layers of these crystals doped with rare earth metals by liquid phase epitaxial growth on substrates of the same family. Among all the crystals of this family, KYW has been probed to be a suitable crystal host for Yb^{3+} doping, at least up to concentrations needed for lasing experiments with high efficiency [7].

Monoclinic KYW crystallizes with a $C2/c$ space group and cell parameters $a = 10.6313(4)$ Å, $b = 10.3452(6)$ Å, $c = 7.5547(2)$ Å, $\beta = 130.752(2)°$ and $Z = 4$ [8].

In the present paper, we discuss the suitable conditions to obtain $KY_{1-x}Yb_x(WO_4)_2/KY(WO_4)_2$ (hereafter $KY_{1-x}Yb_xW/KYW$) by liquid phase epitaxy (LPE). The evolution of lattice mismatch has also been calculated from room temperature to 1273 K. Spectroscopic studies of these crystals, such as optical absorption and emission, are also carried out as a prior study to laser experiments.

2. Experimental details

2.1. Solubility curves

The knowledge of the solubility curve of the solute in a suitable solvent is very important for choosing the composition of

the solution from which the crystal growth will take place. The $K_2W_2O_7$ solvent has been proved as the best known option to grow KREW bulk tungstates by TSSG because, in relation to other solvents, it has several advantages such as low melting temperature and the absence of foreign ions that could be incorporated into the crystal [9]. Other solvents such as K_2WO_4 [10] were used as well, but they introduce a rather high viscosity into the solution as well as creeping problems. In a previous work of some authors of this paper, $K_2W_2O_7$ was proved to be a suitable solvent for the growth of epitaxial layers of KLuW [11]. In the literature, it can be found that Yb:KYW epitaxial layers were grown using a ternary NaCl–KCl–CsCl solvent, but use of this solvent leads to a precipitation of yttrium and tungsten containing oxides [12]. Before the LPE experiments, we determined the solubility curve of $KY_{0.80}Yb_{0.20}(WO_4)_2$ in the solvent $K_2W_2O_7$.

The solubility experiments were carried out in 25 cm^3 platinum crucibles located inside a vertical cylindrical furnace with a Kanthal heater. The temperature was controlled with an 818 P controller/programmer connected to a thyristor. The reagents used were K_2CO_3 (99% purity), Y_2O_3 (99.9% purity), Yb_2O_3 (99.9% purity) and WO_3 (99.9% purity). The solution weights were 15–25 g. After homogenizing the solution, the temperature of the furnace was decreased at a rate of 10 K every 30 min until crystals on a platinum rod were observed. After this, the temperature of saturation of the solution was determined more accurately by increasing/decreasing the temperature of the furnace and observing if there was dissolution or growth of the crystals nucleated on the platinum rod. The crystals obtained were identified by observation with an optical microscope and by x-ray powder diffraction.

2.2. Substrate crystal growth

In order to obtain substrates with a structure as close as possible to the structure of the epitaxial layers, monoclinic crystals of KYW were grown by the top seeded solution growth–slow cooling (TSSG-SC) method. Supersaturation was obtained by slow cooling of the solution from the saturation temperature. The crystal growth was carried out using $K_2W_2O_7$ as solvent.

The experiments were carried out in a cylindrical vertical furnace. The temperature control was achieved with a Eurotherm 903 P controller/programmer connected to a thyristor.

The substrates were grown from about 200 g of solution prepared in 125 cm^3 cylindrical platinum crucibles and the reagents were K_2CO_3, Y_2O_3 and WO_3 with the same purity as the ones used for the solubility curves. The solution composition was 12 mol% KYW/88 mol% $K_2W_2O_7$ and was chosen taking into account the solubility curve of KYW in this solvent [13]. The axial temperature gradient in the solution was 1.5 K cm^{-1}, with the surface cooler than the bottom to avoid the nucleation of crystals at the bottom of the crucible.

Two kinds of crystal growth experiments were carried out. First, we simultaneously grew three crystals located at the surface of the solution about 1 cm from the center and equally spaced. The orientation of these crystals was with the ***b*** direction perpendicular to the surface of the solution. The aim of these crystal growth runs was to obtain small crystals (about 5 mm as maximum dimension) to be used as grown as substrates and to study the epitaxial growth on different crystal faces. In the second kind of runs, we grew a unique single crystal in every experiment with ***b*** crystallographic direction perpendicular to the surface of the solution and located at the center of the solution surface. The crystals obtained in these last experiments were big enough to be cut into plates perpendicular to the ***b*** direction to use as substrates in the epitaxial growth. In both cases, the solution temperature was decreased at a rate of 0.1–0.2 K h^{-1} for 20–28 K from the saturation temperature. The crystal rotation was 40 rpm in all the experiments. After the growth process, they were removed from the solution and maintained just above the surface of the solution, while the furnace was cooled at a rate of 25–30 K h^{-1} to avoid thermal stresses.

2.3. Unit cell parameter

The unit cell parameters of $KY_{1-x}Yb_xW$ for different levels of substitution of Y by Yb (different values of x) were refined from the x-ray powder diffraction data. The crystals needed were obtained with the same procedure as the ones of the solubility curve. For these measurements, we used a Siemens D-5000 powder diffractometer, with Bragg–Brentano parafocusing geometry and vertical θ–θ goniometer. The x-ray powder diffraction patterns were recorded at $2\theta = 10°$–$70°$ with a step size of 0.02° and a step time of 16 s. The cell parameters were refined using the Fullprof program [14].

The change of the cell parameters of undoped KYW and $KY_{0.80}Yb_{0.20}W$ with the temperature was obtained from the x-ray powder diffraction data obtained using the same diffractometer, equipped with an Anton-Paar HTK10 high temperature chamber, over the range between room temperature and 1273 K. The x-ray powder diffraction patterns were recorded at $2\theta = 10°$–$70°$, with a step size of 0.03° and a step time of 5 s. The x-ray patterns were recorded at 298, 323 and 373 K. After this, the time interval between measurements was of 100 K up to 1273 K. The cell parameters were also refined with the Fullprof program.

2.4. Liquid phase epitaxy

The liquid phase epitaxy experiments were carried out in a special furnace with a wide isothermal zone to achieve a thermal gradient in the solution of practically zero. This thermally stable zone contributes to the homogeneous growth over the entire surface of the substrate where the growth process occurs. The LPE experiments were carried out using cylindrical platinum crucibles 30 mm in diameter and 40 mm high. The solution weighed about 70 g. The reagents were the same as in the growth of the substrates and Yb_2O_3 (99.9% purity) for substitution. Different solution compositions were used in these experiments, ranging from 5 mol% $KY_{1-x}Yb_xW$/95 mol% $K_2W_2O_7$ to 12 mol% $KY_{1-x}Yb_xW$/88 mol% $K_2W_2O_7$ in order to study the influence of the solute concentration on the epitaxial growth. Different solution compositions lead to a difference in the slope of the

solubility curve. The chosen solute/solvent composition has to compromise between the rate of growth and the macrodefect density in the epilayer/substrate interface. A small slope in the solubility curve lead to a high solute deposition with small temperature fluctuations, and this fact could involve the appearance of defects in the interface. In contrast, a high slope in the solubility curve involves a low growth rate and the crystal growth is less affected by temperature fluctuations.

The saturation temperature of the solution as well as the kinetics of growth/dissolution at temperatures slightly below/above the temperature of saturation were determined accurately with a KYW seed in contact with the surface of the solution rotating at 40 rpm. These measurements were important to decide the growth conditions of the epitaxial layers [15].

In order to study the influence of the crystalline face on the quality and thickness of the epitaxial layer, LPE experiments on as-grown KYW substrates were carried out. A second kind of experiment, made with (010) oriented plates, was carried out in order to study how the time of growth, solution composition and supersaturation affected the quality and thickness of the epitaxial growth. These plates were obtained by cutting a KYW single crystal in slices 2 mm thick. After this, these plates were polished to optical grade quality and were mounted in a vertical position with platinum wires on an alumina rod.

Before being introduced to the furnace, the substrates were carefully cleaned by dipping them for 5 min in HNO_3/distilled $H_2O = 1/1$. After this, they were dipped for 5 min in distilled water and 5 min in C_2H_5OH. The entire cleaning process was carried out with the crystal in rotation.

The first LPE experiments were carried out using the same solution composition as the growth of the substrates, only substituting some of the Y_2O_3 by Yb_2O_3 in different proportions. After this, we decreased the solute concentration in the solution in order to study its influence on the quality of the layers. The experiments carried out are summarized in Tables 1 and 2. The solute concentrations and Yb contents in the solution are shown in these tables. Also, there are temperatures below the saturation temperature where the LPE crystal growth was carried out and the time of growth. In all the experiments, the surface of the substrates was first dissolved slightly by maintaining the temperature of the solution 1 °C above the saturation temperature for 5 min. After this, the temperature was decreased to the growth temperature. In addition, all the LPE crystal growth experiments were carried out with the substrate rotating at 40 rpm. Finally, the crystals were removed from the solution and taken out of the furnace slowly in order to avoid thermal shocks that could produce cracks in the crystal.

Experiments 1–5, 9 and 12 in as-grown substrates (table 1) and experiments 23 and 27 in (010) slices (table 2) were designed to study the influence of the Yb concentration in the solution on the LPE crystal growth. Experiments 5–11 and 20–22 in as-grown substrates (table 1) and experiments 23–26 and 28 in (010) slices (table 2) were designed for studying the influence of the time of growth on the quality and the thickness of the epitaxial growth. Experiments 9–10, 14–16 and 17–19 in as-grown crystals (table 1) were carried out for studying the influence of the growth temperature, and consequently supersaturation, on the epitaxial crystal growth.

Table 1. Experiments of LPE growth on as-grown substrates and growth conditions.

Experiment number	Solute/ solvent (molar ratio)	Yb content in solution (mol%)	ΔT_{growth} (K)	Growth time (h)
1	12/88	0	−2	2
2	12/88	1	−2	2
3	12/88	2.5	−2	2
4	12/88	5	−2	2
5	12/88	7.5	−2	2
6	12/88	7.5	−2	3
7	12/88	7.5	−2	4
8	12/88	10	−2	1
9	12/88	10	−2	2
10	12/88	10	−1	2
11	12/88	10	−1	4
12	12/88	100	−2	2
13	12/88	100	−1	2
14	7/93	20	−1	4
15	7/93	5	−3	4
16	7/93	5	−6	4
17	5/95	10	−2	2
18	5/95	10	−3	2
19	5/95	10	−4	2
20	5/95	20	−2	2
21	5/95	20	−2	3
22	5/95	20	−2	4

The compositions of the layers obtained by LPE were measured by electron probe microanalysis (EPMA) using a Cameca SX 50. These measurements also allowed us to detect the layer/substrate interface by a compositional change and to measure the thickness of the layer. But because the use of this method to measure the layer thickness requires a lot of EPMA measurements, we only used it in a few cases. The thickness of the epitaxial layers was also measured with an Olympus optical microscope (magnification 5×, 10×, 20× and 50×) using transmission light and by scanning electron microscope (SEM) using backscattered electrons.

The quality of the layer on every crystal face as a function of the solution composition and growth conditions was studied by observing the crystals first with the optical microscope mentioned above and after this with confocal and interferometric microscopy to obtain information on the growth morphologies.

2.5. Spectroscopic study

The optical polarized absorption with $E \parallel N_m$ at room temperature of a $KY_{0.81}Yb_{0.19}W$/KYW(010) epitaxial layer was measured in the 900–1050 nm range, using a Cary Variant 500 spectrophotometer, with a Glan–Taylor polarizer. Fluorescence was dispersed through an HR 460 Jovin Yvon–Spex monochromator and detected by a cooled Hamamatsu R5509-72 NIR. The fluorescence spectra were measured in 90° geometry with a laser diode, emitting at 940 nm, as the excitation source. We analyzed the luminescence signal using an EG&G 7265DPS lock-in amplifier. The sample was

Table 2. Experiments of LPE growth on (010) plates and growth conditions.

Experiment number	Solute/solvent (molar ratio)	Yb content in solution (mol%)	ΔT_{growth} (K)	Growth time (h)
23	5/95	10	−2	2
24	5/95	10	−2	3
25	5/95	10	0/−2	Ramp 0.5 K h^{-1} during 2 h
26	5/95	10	−2	0.5/1/1.5/2
27	5/95	20	−2	2
28	7/93	20	−6	2/3/4/5/8/12/20/22/24

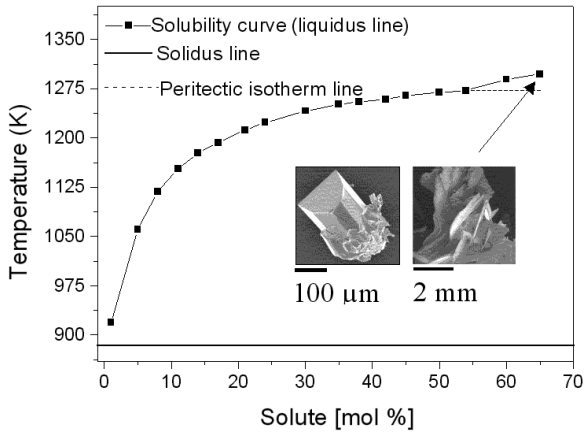

Figure 1. Solubility curve of $KY_{0.80}Yb_{0.20}W$ in the solvent $K_2W_2O_7$. The insets show on the left a photograph of the crystal habit of the monoclinic phase, and on the right a photograph of the layered crystal habit.

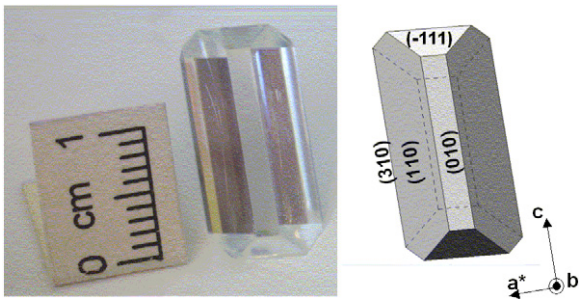

Figure 2. KYW single crystal before being cut in slices for substrates and a crystal scheme obtained with the Shape program.

pumped along the ***c*** crystallographic axis, and the emitted light was collected parallel to the ***b*** direction.

Lasing experiments were carried out using $KY_{0.81}Yb_{0.19}W$/KYW with a layer of 48 μm grown from a solution with 20 mol% of Y substituted by Yb. Continuous-wave lasing at 1030 nm with an output power of 40 mW was obtained at room temperature. More details of laser experiments can be seen in [16].

3. Experimental results and discussion

3.1. Solubility curves

Figure 1 shows the solubility curve of $KY_{0.80}Yb_{0.20}W$ in the solvent $K_2W_2O_7$. Compared with those of KYW and KYbW, published elsewhere [13, 17], it can be said that there was no significant difference in their solubility. At around 54% solute composition and 1273 K, there appears a drastic change in the slope of the solubility curve. After this point, the $C2/c$ monoclinic morphology leads to layered crystals corresponding to orthorhombic high temperature phase isostructural to $KY(MoO_4)_2$ [18–20]. The insets in figure 1 show a photograph of both crystal habits that appeared: the monoclinic and the layered one. The solidus line is located at 884 K and indicates the temperature below which the solution turns solid for any composition.

In the solubility curve shown in figure 1, we can observe two regions with very different slopes. From 5 to about 15 mol% solute, the solubility curve has a higher slope than for solute concentrations above 15 mol%. From these results, we concluded that solutions with solute concentration lower than 15 mol% are, *a priori*, the most suitable for single crystal and epitaxial growth since the supersaturation of the solution would be less affected by temperature fluctuations.

3.2. Substrate crystal growth

As mentioned in the experimental details, two kinds of substrates were used: as-grown substrates and slices perpendicular to the (010) direction cut from bulk crystals and polished. The crystals obtained in the two kinds of crystal growth runs were transparent, colorless and free from inclusions and other macroscopic defects.

The crystals with dimensions less than 5 mm were used for substrates without any other treatment, only careful cleaning. These KYW single crystals are formed by the {110}, {010}, $\{\bar{1}11\}$ and {310} faces as can be seen in figure 2, where a photograph is shown of a crystal and a morphological scheme obtained with the Shape program [21].

The bulk crystals to be cut in slices weighed between 3.0 and 6.3 g and their dimensions were in the range 7–9.1 mm × 6.9–9.2 mm × 13.6–19.8 mm in $\boldsymbol{a}^* \times \boldsymbol{b} \times \boldsymbol{c}$ directions. These crystals were cut with a diamond saw and polished to obtain (010) slices with minimum deviation from this direction and a roughness less than 3 μm.

Table 3. Cell parameters of KYW and $KY_{1-x}Yb_xW$.

$[Yb]_{solution}$ (at.%)	a (Å)	b (Å)	c (Å)	β (deg.)	Volume (Å^3)
0	10.6313(4)	10.3452(6)	7.5547(3)	130.752(2)	629.44(5)
5	10.6250(5)	10.3380(5)	7.5475(3)	130.745(2)	628.09(5)
10	10.6239(5)	10.3326(5)	7.5448(3)	130.745(3)	627.48(5)
20	10.6200(6)	10.3213(6)	7.5382(4)	130.744(3)	625.98(6)
50	10.6098(5)	10.2952(5)	7.5223(4)	130.751(3)	622.45(5)
100	10.6003(12)	10.2673(12)	7.5066(8)	130.766(6)	618.78(12)

Table 4. Mismatch between $KY_{1-x}Yb_xW$ layers and KYW substrate.

Composition	$f_{(010)}$	$f_{(110)}$	$f_{(310)}$	$f_{(\bar{1}11)}$
$KY_{0.95}Yb_{0.05}W$/KYW	−0.1440	−0.1570	−0.1635	−0.1283
$KY_{0.90}Yb_{0.10}W$/KYW	−0.1901	−0.2290	−0.2487	−0.1863
$KY_{0.80}Yb_{0.20}W$/KYW	−0.3125	−0.3974	−0.4403	−0.3252
$KY_{0.50}Yb_{0.50}W$/KYW	−0.6287	−0.8038	−0.8923	−0.6745
KYbW/KYW	−0.9473	−1.2195	−1.3572	−1.0397

3.3. Unit cell parameters

Before carrying out the LPE experiments, the change of the cell parameters with the Yb contents in the crystal was determined because of its relation to the defect generation in the film/substrate interface of the composite.

Table 3 shows the unit cell parameters of KYW and $KY_{1-x}Yb_xW$ for different levels of substitution of Y by Yb. As a consequence of the minor ionic radius of Yb^{3+} (0.985 Å) with respect to the ionic radius of Y^{3+} (1.019 Å) [22], the cell parameters decrease when the Yb concentration increases, except for the angle $\boldsymbol{\beta}$, that within experimental error is practically constant. The change in $\boldsymbol{b}$ parameter is more significant than the change in $\boldsymbol{a}$ and $\boldsymbol{c}$ parameters. Consequently, the cell volume also decreases with increasing of Yb.

A bidimensional lattice mismatch can be defined by the expression $f_{(hkl)} = [(S_{L(hkl)} - S_{S(hkl)})/S_{S(hkl)}] \times 100$, where $S_{S(hkl)}$ and $S_{L(hkl)}$ are the areas of the (hkl) periodicity vectors of the substrate and the layer, respectively. Table 4 summarizes the lattice mismatches for the {010}, {110}, {310} and $\{\bar{1}11\}$ faces at room temperature. The same mismatches are represented in figure 3. High mismatches between the layer and the substrate will lead to a high stress in the interface that could produce cracks [16]. It can be said that, up to 10 at.% of Yb substituting Y in the layer, the face with the lowest mismatch between the layer and the substrate is the $(\bar{1}11)$ face, while for higher Yb concentrations the face with the lowest mismatch is the (010) face. The layer on the (110) face has a higher mismatch than the layer on the (010) face, but lower than the one on the (310) face. In addition to having a low mismatch, the (010) face also has a low rate of growth, which could be the reason why the epitaxies on this face generally have a high level of flatness and few defects. Moreover, the (010) face is the most interesting one for optical applications due to the fact that the principal optical axes $\mathbf{N_g}$ and $\mathbf{N_m}$ are contained in the a–c plane perpendicular to the (010) direction.

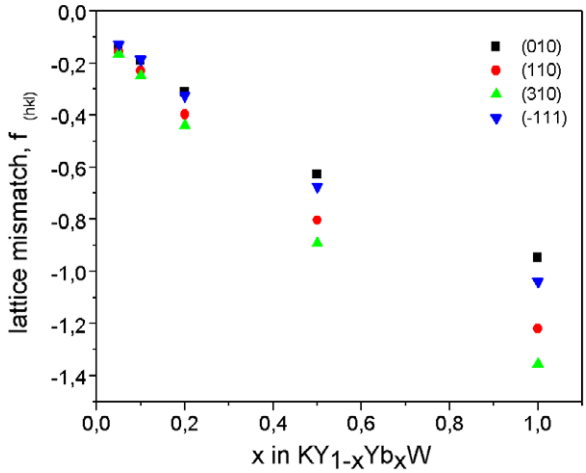

Figure 3. Lattice mismatch between $KY_{1-x}Yb_xW$ layers and KYW substrates.

3.4. Lattice mismatch variation with temperature

Since the thermal expansion of the epilayer and the substrate are not equal (figures 4(a) and (b)), the lattice mismatch is not constant as the temperature varies. The thermal evolution of the lattice mismatch between the substrate and the epilayer, KYW and $KY_{0.80}Yb_{0.20}W$, respectively, is presented in figure 4(c).

The linear thermal expansion coefficients in a given crystallographic direction are $\alpha = (\partial L/\partial T)/L$, where L is the initial parameter at 298 K and ΔL is the change in this parameter when the temperature is changed by ΔT. The α_{ij} are the slopes and conform the linear thermal expansion tensor in the crystallophysical frame. Using the experimental data of figure 4(a), the linear thermal expansion values for $KY_{0.80}Yb_{0.20}W$ are $\alpha_{100} = 10.5 \times 10^{-6}(K)^{-1}$, $\alpha_{010} = 2.77 \times 10^{-6}(K)^{-1}$, $\alpha_{001} = 18.3 \times 10^{-6}(K)^{-1}$, $\alpha_{c^*} = 20.7 \times 10^{-6}(K)^{-1}$ and $\alpha_V = 30.0 \times 10^{-6}(K)^{-1}$. By diagonalizing this tensor, we obtained a linear thermal expansion tensor in the principal system X'_1, X'_2, X'_3. The linear thermal expansion tensor values in the principal system are $\alpha'_{33} = 21.1 \times 10^{-6}\ K^{-1}$, X'_3 found at 30.2° rotating anti-clockwise from the $\boldsymbol{c}$ axis with the $\boldsymbol{b}$ positive axis pointing towards us; $\alpha'_{11} = 10.1 \times 10^{-6}\ K^{-1}$ for the X'_1 principal direction and $\alpha'_{22} = 20.7 \times 10^{-6}\ K^{-1}$ for the X'_2 ($\boldsymbol{b}$ crystallographic direction) principal axis. Comparing these values to the previously published ones for KYW in [8], it can be observed that these values are higher, and this fact implies a greater dilatation of the epilayer than the substrate when increasing the temperature.

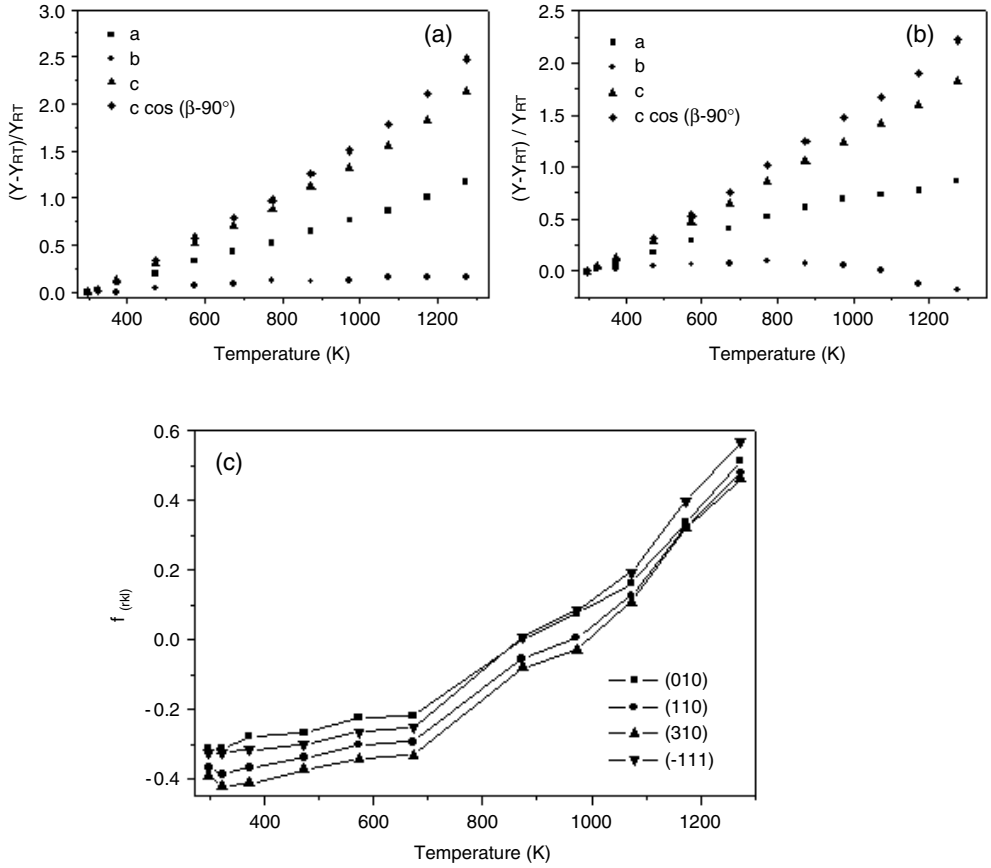

Figure 4. (a) Thermal evolution of unit cell parameters of $KY_{0.80}Yb_{0.20}W$ and (b) KYW and (c) lattice mismatch.

An $f_{(hkl)} > 0$ indicates a tensile strain, while an $f_{(hkl)} < 0$ implies a compressive strain in the composite interface. Figure 4(c) shows the evolution of the lattice mismatch from room temperature to 1273 K. As can be seen, the values of $f_{(hkl)}$ are around 0.6% at higher temperature where the growth process occurs and decrease as the temperature does. So, a very slow cooling ramp once the epitaxial sample is grown and extracted from the solution will be needed until around 773 K to avoid interface defects due to the high difference between the epitaxial and substrate lattice parameters. Below this temperature, the cooling ramp rate can be faster because the lattice mismatch difference is rather low. As can be seen, the thermal evolution of lattice mismatch is very similar for all the faces studied.

3.5. Liquid phase epitaxy

The LPE experiments using as-grown substrates to study the quality of the epitaxies grown on the different crystal faces and LPE on (010) plates are summarized in tables 1 and 2, respectively. The dissolution of the surface of the substrates at 1 K above the saturation temperature over 5 min has proven that there is no contribution to the increase of the defects in the interface, since it only dissolves the outer part of the crystal in order to eliminate possible surface defects.

For a 5 at.% Yb substitution, the mismatch between the layer and the substrate on the (010) face is small enough to permit the growth of the layer on the substrate with a high flatness. For substitutions of Y by Yb higher than 10 at.%, the tendency for defects to appear in the interface is increased. The layer/substrate mismatch on the $(\bar{1}11)$ face is of the same order as on the (010) face but the layers on the $(\bar{1}11)$ face were generally of poor quality. One possible explanation is that this face has a growth rate higher than its neighbor faces and this can contribute to the occurrence of more defects in the layer. The layers grown on the (110) face generally have a high quality of up to 10 mol% of substitution of Y by Yb because the mismatch is also small in this case. Finally, the layers obtained on the (310) faces generally have more defects than the layers grown on (010) and (110) faces but less than the layers grown on $(\bar{1}11)$ faces. So, for the following studies, only (010) oriented slices were used. As an example, figure 5 shows photographs of LPE layers grown on different crystal faces, where we can observe the typical growth defects on these faces.

The Yb concentration in the growth solution has a significant influence on the quality of the layers. Thus, using the growth conditions of this work, we have observed that in some of the experiments there is a tendency for some cracks to begin appearing in the layer/substrate interface of the crystal when the substitution of Y_2O_3 by Yb_2O_3 in the solution is 10 mol%. By increasing the substitution to 20 mol%, even with low solute concentration in the solution, the cracks are present in equal distribution in the layer/substrate interface

Table 5. Layer thickness of $KY_{1-x}Yb_xW$/KYW grown from 12 mol% solute a 10 mol% of Y substituted by Yb in solution.

Experiment number	Growth time (h)	ΔT_{growth} (K)	(010) face Thickness (μm)	(110) face Thickness (μm)	(310) face Thickness (μm)
8	1	−2	63	32	14
9	2	−2	77	50	20
10	2	−1	68	46	16
11	4	−1	103	48	25

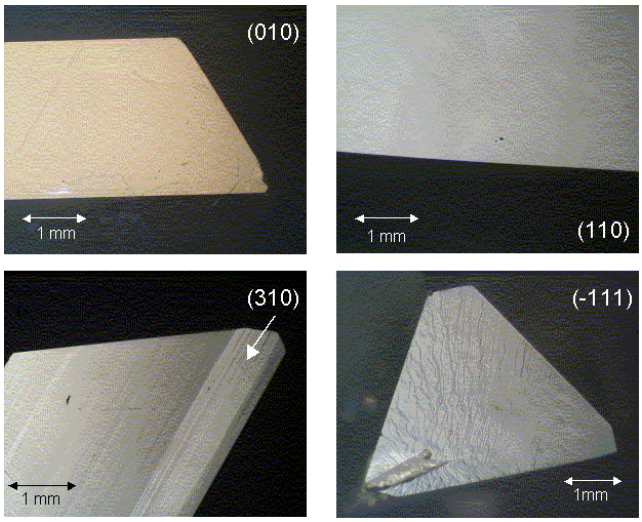

Figure 5. Typical growth defects on several crystal faces.

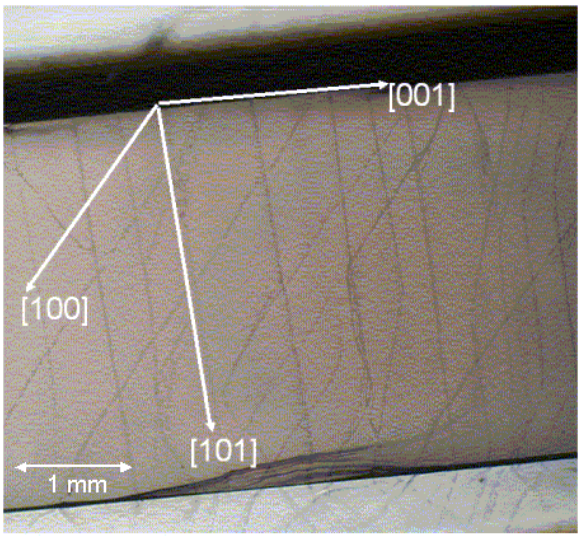

Figure 6. Morphologies in the layer/substrate interface that appeared for a sample with 20 mol% of Y substituted by Yb in the epitaxial layer.

(see figure 6). In the epitaxial growth of KYbW/KYW, the interface defects are so important that they make the samples not transparent (experiments 12 and 13), probably due to the high lattice mismatch between the layer and the substrate.

The most commonly observed morphologies in the layers are growth steps, which were first observed by optical microscope and after this by confocal and interferometric microscopy. Figure 7 shows, as an example, a confocal image of representative $KY_{0.95}Yb_{0.05}W$/KYW and $KY_{0.80}Yb_{0.20}W$/KYW layers grown on (010) faces with the same z-axis scale. Both samples were grown from a 7 mol% solute solution at a temperature 2 K below the saturation temperature; the growth time was 4 h and the crystal rotation 40 rpm. As can be seen in the figure, the rms (root mean square) roughness of the $KY_{0.80}Yb_{0.20}W$/KYW sample is clearly higher than that of the $KY_{0.95}Yb_{0.05}W$/KYW one, 490 and 160 nm respectively. In the profiles, there can also be observed a greater height in the growth steps. In the case of the $KY_{0.80}Yb_{0.20}W$/KYW epitaxial sample, there can be observed a high number of growth centers in the form of growth hillocks, which were more active than centers which had dominated the growth process over the whole face. These growth centers may be mainly due to solution remains in the surface of the crystal. Surface cracks are a source for solution which leads to the structures shown in the inset of figure 7(b).

The increase of the thickness of the epitaxial growth on the (010) face as a function of the growth time was studied (experiments 26 and 28). First, we dipped the crystal into the solution several millimeters, followed by pulling the crystal in steps of 1 mm at known intervals of time (30 min in experiment 26 and longer times in experiment 28). In the final pull, we entirely removed the crystal from the solution. Figure 8 shows the evolution of the layer thickness on the (010) crystal face with the time of growth and the average growth rates at 6 and 22 h. The thickness increases almost linearly until around 10 h at 19.5 μm h^{-1} and then the rate decreases to 2.4 μm h^{-1} at 22 h. Comparing these growth rates with those previously published for $KLu_{0.78}Yb_{0.22}W$/KLuW [11], it can be observed that the growth rates for $KY_{0.80}Yb_{0.20}W$/KYW are much higher. This effect may be due to the higher value of lattice mismatch between the epilayer and the substrate, which induces a higher number of defects in the interface, leading to an increase in the number of kinks where the growth units can attach.

Table 5 shows the layer thickness of $KY_{1-x}Yb_xW$/KYW grown from 12 mol% solute and 10 at.% of Y substituted by Yb in solution for two different levels of supersaturation and different times of growth. The thicknesses of the faces were evaluated by the observation by SEM of the epitaxy cut perpendicular to the ***b*** crystallographic direction and measuring the distance from the substrate–epilayer interface. This is the reason why the values of $(\bar{1}11)$ thickness are not present in table 5. Of all the faces studied, the face with higher velocity of layer growth is the (010), followed by the (110). The layers

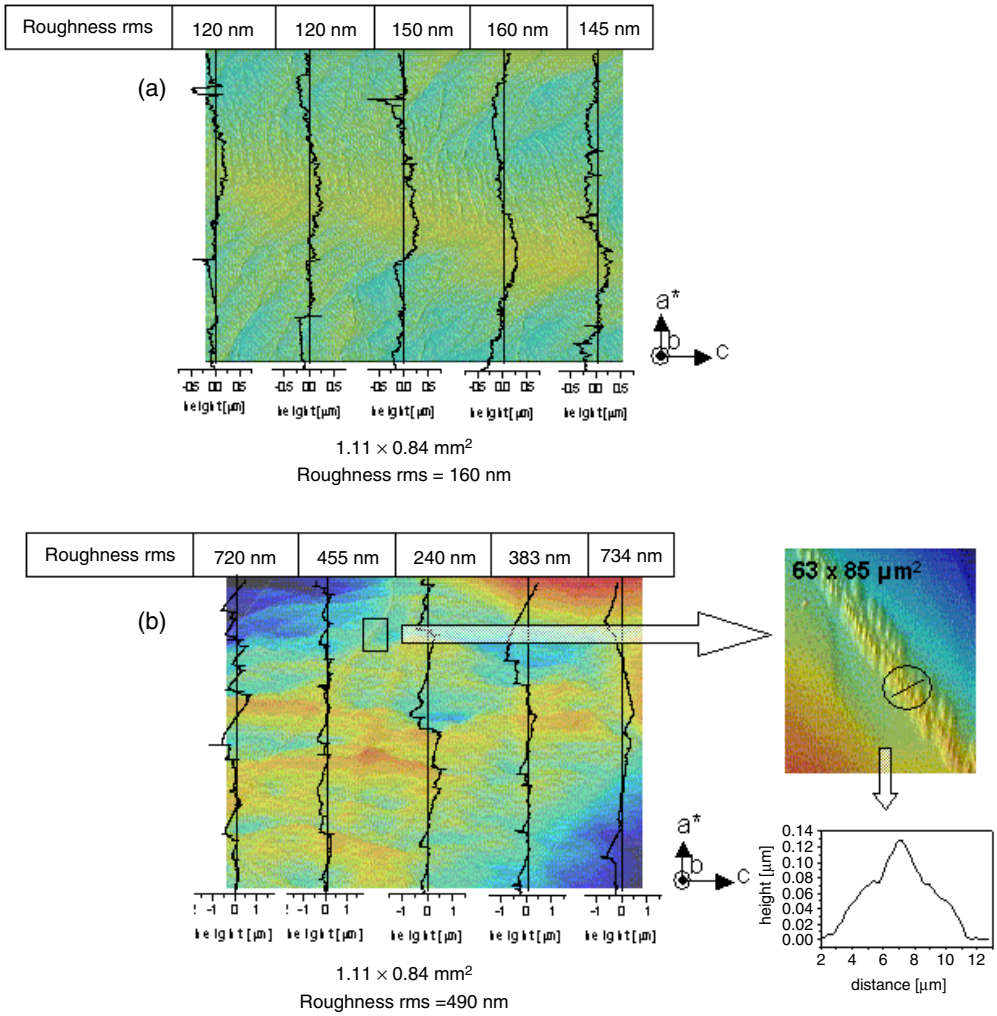

Figure 7. (a) Confocal image of $KY_{0.95}Yb_{0.05}W$/KYW layers grown on a (010) face and (b) $KY_{0.80}Yb_{0.20}W$/KYW layers grown on a (010) face; the detail shows a growth center in the form of a growth hillock.

grown on (010) and (110) faces are generally of higher quality than the layers obtained on the (310) and ($\bar{1}11$) faces.

The solute/solvent ratio in the growth solution slightly influences the growth velocity, but the quality of the layer/substrate is practically unchanged (experiments 9 and 17).

The influence of the growth temperature of the epitaxial layers is studied in experiments 9–10, 14–16 and 17–19. From these experiments, we conclude that at low levels of supersaturation (growing from 2 to 6 K below the saturation temperature, using about 70 g of solution) no significant changes in the quality of the epitaxial growth or in the velocity of growth are observed.

The layer composition was measured by EPMA with wavelength dispersive spectroscopy (WDS) and the distribution coefficient of Yb was calculated according to the expression $K_{Yb} = \{[Yb]/([Yb] + [Y])\}_{layer}/\{[Yb]/([Yb] + [Y])\}_{solution}$, where [Yb] and [Y] are the concentrations of Yb and Y, respectively. Table 6 summarizes the composition of the layers and the distribution coefficient of Yb for different levels of substitution of Y by Yb. We have observed that in the distribution coefficient of Yb there was practically no change with the solute/solvent ratio for the ratios studied in this work. For all the levels of substitution studied, the distribution coefficient of Yb is close to unity.

Table 6. Crystal composition and distribution coefficient of Yb for different levels of substitution.

Solute/solvent (molar ratio)	K_{Yb}	Stoichiometric formula
5	1.03	$KY_{0.95}Yb_{0.05}(WO_4)_2$
10	1.02	$KY_{0.90}Yb_{0.10}(WO_4)_2$
20	0.95	$KY_{0.81}Yb_{0.19}(WO_4)_2$

3.6. Spectroscopic study

In the inset of figure 9 is shown the polarized optical absorption of an oriented $KY_{0.81}Yb_{0.19}(WO_4)_2$/KYW (010) epitaxial layer at room temperature. The light was polarized parallel to the principal optical direction N_m. In this family of materials, the optical absorption of Yb^{3+} strongly depends on the light polarization; in previous studies, the highest absorption values are those reported by Mateos *et al* [23] at 980.6 nm with

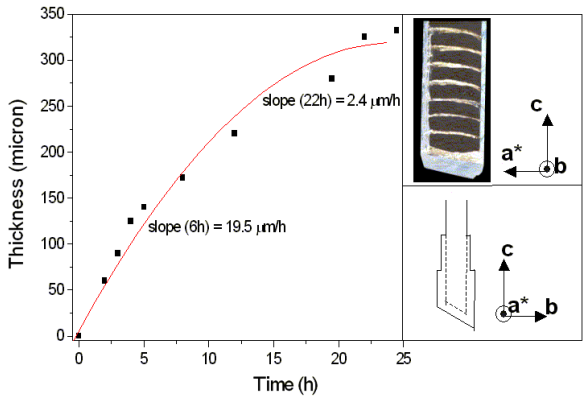

Figure 8. Epitaxial layer thickness versus the time of growth on a (010) slice (experiment number 28) with image and schematic view of the sample.

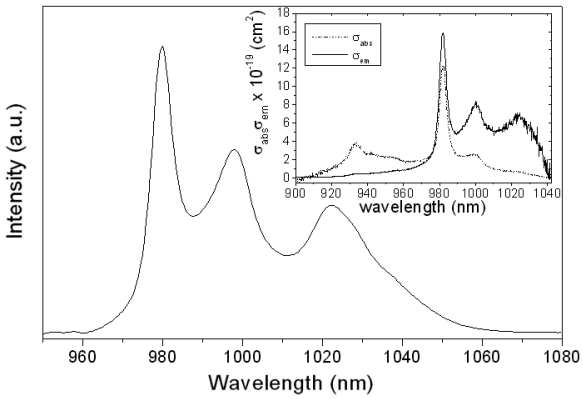

Figure 9. Emission cross-section spectrum of a $KY_{0.81}Yb_{0.19}(WO_4)_2$/KYW crystal. Inset: emission cross-section calculated using the reciprocity method and absorption cross-section spectrum used for the calculations.

$E \parallel N_m$ $\sigma_{abs} = 11.7 \times 10^{-20}$ cm^2 and by Kuleshov *et al* [24] at 981.2 nm with $E \parallel a'$ (where a' is the unit cell parameter expressed in the space group $I2/c$; $a' = (a + c)$, $\boldsymbol{a}$ and $\boldsymbol{c}$ are the unit cell parameters in $C2/c$) and the cross-section value is $\sigma_{abs} = 13.3 \times 10^{-20}$ cm^2.

As can be observed from the spectrum, the $^2F_{7/2} \rightarrow {}^2F_{5/2}$ transition has three main peaks centered at 933.6, 981.8 and 1000.0 nm.

The maximum absorption cross-section σ_{abs} at 981.8 nm, calculated with the Yb^{3+} concentration of 1.992×10^{21} ions cm^{-3}, amounts to 12.5×10^{-20} cm^2. The emission cross-section spectrum was calculated with the reciprocity method using the absorption cross-section spectrum at room temperature and the splitting determined at low temperature in [16]. The results are also included in the inset of figure 9 and compared with the experimental unpolarized emission spectrum obtained in the present paper (see figure 9). The peaks correspond to the transition from the excited $^2F_{5/2}$ level to the four sublevels of the ground state $^2F_{7/2}$.

It is worth mentioning that the relative intensity of the peak at 981.8 nm, corresponding to the $^2F_{5/2}(0') \rightarrow {}^2F_{7/2}(0)$ sublevel transition, shows a slight decrease in the experimental spectrum in comparison with the calculated spectrum. The experimental emission spectrum is an average of N_g and N_m polarized emission spectra as a result of the above described experimental configuration. There is a significant overlap between the absorption and emission spectrum around 982 nm, which can produce reabsorption during lasing experiments. Thin layers minimize this effect [24]. The maximum calculated emission cross-section is 15.8×10^{-20} cm^2 at 982.6 nm.

Efficient continuous-wave laser emission was achieved at around 1030 nm with an output of 40 mW from a sample $KY_{0.81}Yb_{0.19}(WO_4)_2$/KYW (010) epitaxial layer obtained and described in the present paper. More details of the laser operation can be found in [16].

4. Conclusions

Epitaxial layers of $KY_{1-x}Yb_x(WO_4)_2/KY(WO_4)_2$ were grown by liquid phase epitaxy on bulk substrates and (010) slices. It has been proved that a growth temperature up to 6 K below the saturation temperature is useful to obtain high quality epitaxial layers. From solute concentration in the range from 5 to 12 mol%, no significant changes in the quality of the epilayers has been observed.

The layers grown from solutions of up to 7.5 at.% of Y substituted by Yb are generally of high quality, principally on faces (010) and (110). For substitutions higher than this, some cracks at the layer/substrate interface begin to appear. The layers grown on (310) and ($\bar{1}11$) are generally of worse quality than the layers on the (010) and (110) faces. The face with highest velocity of growth is the (010) face. No significant increase in the growth velocity of the layer with the level of supersaturation, for the low levels of supersaturation studied in this work, was observed.

The optical absorption with $E \parallel N_m$ polarization shows three main absorption peaks corresponding to the $^2F_{7/2} \rightarrow {}^2F_{5/2}$ transition centered at 933.8, 981.8 and 998.4 nm and a maximum absorption cross-section of 12.5×10^{-20} cm^2.

Acknowledgments

This work was supported by the EU project DT-CRYS, NMP3-CT-2003-505580, by the Ministerio de Educación y Ciencia projects MAT2004-20471-E, MAT-2005-06354-C03-2 and CIT-020400-2005-14 and by the Generalitat de Catalunya project 2005SGR658.

References

[1] Innerhofer E, Südmeyer T, Brunner F, Häring R, Aschwanden A, Paschotta R, Hönninger C, Kumkar M and Keller U 2003 *Opt. Lett.* **28** 367–9
[2] Zou X and Toratani H 1995 *Phys. Rev.* B **52** 15889–97
[3] Brunner F, Südmeyer T, Innerhofer E, Morier-Genoud F, Paschotta R, Kisel V E, Shcherbitski V G, Kuleshov N V, Gao J, Contag K, Giesen A and Keller U 2002 *Opt. Lett.* **27** 1162–4
[4] Pujol M C, Solé R, Nikolov V, Gavaldà J, Massons J, Zaldo C, Aguiló M and Díaz F 1999 *J. Mater. Res.* **14** 3739–45

[5] Griebner U, Liu J, Rivier S, Aznar A, Grunwald R, Solé R, Aguiló M, Díaz F and Petrov V 2005 *IEEE J. Quantum Electron.* **41** 408–14
[6] Mateos X, Solé R, Gavaldà J, Aguiló M and Díaz F 2005 *J. Lumin.* **115** 131–7
[7] Lagatsky A A, Kuleshov N V and Mikhailov V P 1999 *Opt. Comunn.* **65** 71–5
[8] Pujol M C, Mateos X, Solé R, Gavaldà J, Massons J, Aguiló M and Díaz F 2001 *Mater. Sci. Forum* **378–381** 710–7
[9] Solé R, Nikolov V, Ruiz X, Gavaldà J, Solans X, Aguiló M and Díaz F 1996 *J. Cryst. Growth* **169** 600–3
[10] Klevtsov P V and Kozeeva L P 1969 *Sov. Phys.—Dokl.* **14** 185–7
[11] Aznar A, Silvestre O, Pujol M C, Solé R, Aguiló M and Díaz F 2006 *Cryst. Growth Des.* **6** 1781–7
[12] Romanyuk Y E, Utke I, Ehrentraut D, Apostolopoulos V, Pollnau M, García-Revilla S and Valiente R 2004 *J. Cryst. Growth* **269** 377–84
[13] Tu C, Huang Y, Luo Z and Chen G 1994 *J. Cryst. Growth* **135** 636–8
[14] Rodríquez-Carvajal J 1996 *Reference Guide for the Computer Program Fullprof* Laboratorie León Brilloui, CEA-CNRS, Saclay, France
[15] Solé R, Nikolov V, Vilalta A, Carvajal J J, Massons J, Gavaldà J, Aguiló M and Díaz F 2002 *J. Cryst. Growth* **237–239** 602–7
[16] Aznar A, Solé R, Aguiló M, Díaz F, Griebner U, Grunwald R and Petrov V 2004 *Appl. Phys. Lett.* **85** 4313–5
[17] Pujol M C, Solé R, Massons J, Gavaldà J, Solans X, Díaz F and Aguiló M 2002 *J. Appl. Crystallogr.* **35** 108–12
[18] Klevtsov P V, Kozeeva L P, Kharchenko L Y and Pavlyuk A A 1974 *Sov. Phys.—Crystallogr.* **19** 342–6
[19] Klevtsov P V and Kozeeva L P 1977 *J. Struct. Chem.* **18** 339–55
[20] Klevtsov P V, Kozeeva L P and Kharchenko L Y 1974 *Sov. Phys.—Crystallogr.* **20** 732–5
[21] Dowty E 1995 *Shape for Windows, Version 5.0.1*
[22] Shannon R D 1976 *Acta Crystallogr.* A **32** 751–67
[23] Mateos X, Solé R, Gavaldà J, Aguiló M, Massons J and Díaz F 2006 *Opt. Mater.* **28** 423–31
[24] Kuleshov N V, Lagatsky A A, Podlipensky A V and Mikhailov V P 1997 *Opt. Lett.* **22** 1317–9